Wang et al. BMC Medical Imaging (2025) 25:46
https://doi.org/10.1186/s12880-025-01575-7

BMC Medical Imaging

RESEARCH Open Access

Development and validation of a CT-based radiomic nomogram for predicting surgical resection risk in patients with adhesive small bowel obstruction

Zhibo Wang[1,2], Ling Zhu[3], Shunli Liu[4], Dalue Li[5], Jingnong Liu[1], Xiaoming Zhou[4], Yuxi Wang[6] and Ruiqing Liu[1,7*]

Abstract

Background Adhesive small bowel obstruction (ASBO) is a common emergency that requires prompt medical attention, and the timing of surgical intervention poses a considerable challenge. Although computed tomography (CT) is widely used, its effectiveness in accurately identifying bowel strangulation is limited. The potential of radiomics models to predict the necessity for surgical resection in ASBO cases is not yet fully explored.

Objectives The aim of this study is to identify risk factors for surgical resection in patients with ASBO and to develop a predictive model that integrates radiomic features with clinical data. This model designed to estimate the likelihood of surgical intervention and aid in clinical decision-making for acute ASBO cases.

Methods From January 2019 to February 2022, we enrolled 188 ASBO patients from our hospital, dividing them randomly into a training cohort ($n = 131$) and a test cohort ($n = 57$) using a 7:3 ratio. We collected baseline clinical data and extracted radiomic features from CT images to compute a radiomic score (Rad-score). A nomogram was developed that combines clinical characteristics and Rad-score. The performance of clinical, radiomic, and combined nomogram models was evaluated in both cohorts.

Results Of the 188 patients, 92 underwent surgical resection, while 96 did not. The nomogram integrated factors such as white blood cell count, duration of obstruction, and preoperative infection indicators (fever, tachycardia, peritonitis), along with CT findings (elevated wall density, thickened wall, mesenteric fluid, ascites, bowel wall gas, small bowel feces, and hyperdensity of mesenteric fat) ($p < 0.1$). This combined model accurately predicted the need for surgical resection, with area under the curve (AUC) values of 0.761 (95% CI, 0.628–0.893) for the test cohort. Calibration curves showed strong agreement between predicted and observed outcomes, and decision curve analysis validated the model's utility for acute ASBO cases.

Conclusion We developed and validated a CT-based nomogram that combines radiomic features with clinical data to predict the risk of surgical resection in ASBO patients. This tool offers valuable support for treatment planning and decision-making in emergent situations.

*Correspondence:
Ruiqing Liu
liuruiqing@qdu.edu.cn

Full list of author information is available at the end of the article

Keywords Acute adhesive small bowel obstruction, Radiomics, Surgical resection

Introduction

Small bowel obstruction (SBO) is a common acute abdomen condition, accounting for more than 15% of emergency surgical admissions [1]. Adhesive small bowel obstruction (ASBO) is frequently caused by intraabdominal adhesions, often a consequence of previous surgeries, which induce torsion and angulation of the small bowel [2]. These adhesive bands can compress the small bowel, potentially leading to severe complications such as closed loop formations, strangulation, or even perforation during the course of ASBO [3]. Although most ASBO patients are managed non-operatively, approximately 15% who are admitted to hospitals undergo surgery, making ASBO one of the predominant reasons for small bowel surgeries, including resection, stoma creation, and adhesiolysis [4]. Typically, adhesiolysis is the most common surgical procedure for ASBO, however, between 28% and 45.7% of surgical patients require bowel resection, which is associated with considerable morbidity and mortality [5–7]. In our previous study, postoperative complication rates ranging from 42.31 to 48.87% were observed in ASBO patients who underwent surgical resection, highlighting significant risks [8]. Consequently, surgeons often face challenging decisions regarding the necessity and timing of surgical resection for ASBO patients: operating too early can increase costs compared to nonoperative treatments and expose patients to surgical risks; however, delayed surgery may lead to prolonged hospital stays and increased risks of intra-abdominal sepsis [9]. Clinical evaluations for assessing bowel viability are often inadequate in timing and accuracy.

Currently, several radiologic procedures are available to assist in evaluating the severity of ASBO, with CT imaging being the most utilized method. Previous studies have validated the advantages of CT imaging in diagnosing, locating, and determining the degree of obstruction, with an accuracy of approximately 70% in identifying bowel ischemia [10, 11]. Nonetheless, the effectiveness of abdominopelvic CT in determining surgical indications remains limited [12]. Matsushima et al. developed a radiographic model based on image signs to predict the necessity for surgical intervention, yet only 10% of patients requiring surgery exhibited the relevant CT findings [13]. Moreover, most previous studies focused primarily on analyzing the relationship between typical CT characteristics and surgical risk, yet these characteristics often appear on CT images only after ASBO has progressed significantly, failing to timely indicate the pathological status of the intestinal tract and potentially causing surgeons to miss the optimal timing for resection of necrotic intestine [14, 15]. Thus, to date, no practical image-based tool effectively predicts the risk of surgical resection at an early stage of ASBO.

In recent years, radiomics has emerged as a novel method for quantifying disease changes through data mining of images and has been widely validated in clinical imaging. This innovative technique extracts quantitative parameters that are imperceptible through visual inspection, using high-throughput technology from images, and enhances decision-making [16]. Radiomic models are increasingly utilized for diagnosing diseases and predicting the prognosis of cancer, such as the preoperative prediction of metastasis or recurrence in gastrointestinal cancers [17]. We previously developed a radiomic model using 167 CT enterography images from Crohn's disease (CD) cases and achieved good performance in predicting the inflammatory severity of bowel segments in CD patients [18]. Consistent with a series of studies [18, 19], our results underscored the potential usefulness of radiomics in evaluating benign diseases. ASBO, characterized as a benign disease, involves diseased bowel segments whose histopathological changes can be depicted in CT imaging. Thus, we speculate that applying radiomics to predict the surgery risk of ASBO holds promise.

Based on this premise, this study screened clinical risk factors related to the surgical resection risk of ASBO from intraoperative findings, clinical data, and blood biochemical indices, and extracted imaging features of obstructive diseased lesions using radiomic methods. An integrative radio-clinic model was constructed, combining novel imaging features, which is easily applied clinically and provides a crucial basis for rational decision-making in the treatment of ASBO.

Materials and methods

The CLEAR checklist was used for guiding the reporting of current study and is presented in a Supplementary Table S1 [20]. The overall quality of the pipeline was assessed by the METhodological RadiomICs Score (METRICS) tool [21], with a METRICS score of 82.1% (Supplementary Table S2). This retrospective study was approved by the Ethics Committee of the Affiliated Hospital of Qingdao University (QYFYWZLL26445).

Patients

The researchers followed all the rules laid out in the Declaration of Helsinki. Patients diagnosed with ASBO who underwent surgery between January 2019 and February 2022 were retrospectively identified. Surgical resections were indicated when intraoperative findings suggested compromised bowel viability, such as signs of prolonged ischemia or necrosis. A total of 188 cases were included, comprising patients who underwent surgical resection and those who did not. These cases were randomly divided into a training cohort ($n = 131$) and a test cohort ($n = 57$) at a 7:3 ratio. The randomization process was presented in Supplementary materials A1. Inclusion criteria included: (1) diagnosis of ASBO based on clinical, histological, or radiological findings; (2) history of abdominal surgeries; (3) emergent surgery due to ASBO; and (4) preoperative abdominal CT scans obtained within 24 h of admission. Exclusion criteria included: (1) admission to a non-emergency department; (2) incomplete surgical reports or missing clinical data; (3) bowel obstruction due to primary tumors, hernias, acute mesenteric vascular embolism, ischemic bowel disease or inflammatory bowel disease; and (4) age under 18 years. The patient selection flowchart is shown in Supplementary Figure S1.

Baseline Clinical Data Collection

Baseline clinical data were collected according to established protocols and included sex, age, body mass index (BMI), presenting symptoms (defecation issues, vomiting, abdominal pain), history of previous abdominal surgeries, time to obstruction, American Society of Anesthesiologists (ASA) score, signs of abdominal sepsis, and laboratory indicators (white blood cell count, platelet count, hemoglobin, albumin, and C-reactive protein levels). Typical CT features associated with surgical resection, as identified in prior studies [11, 22–23], included elevated wall density, wall thickening, mesenteric fluid, ascites, bowel wall gas, small bowel feces, free air, hyperdensity, and whirlpool sign of mesenteric fat. Two experienced radiologists, blinded to the clinical outcomes, reviewed the CT images using the predefined criteria (Supplementary Table S3 and Figure S2).

CT image evaluation

CT scans were performed within 24 h of emergent admission using two scanners: Somatom Sensation 64 (Siemens Healthcare) and Discovery 750 (GE Healthcare). Scanning parameters included a tube current of 200 mA, tube voltage of 120 kV, matrix size of 512×512, pitch of 0.8, and a section thickness of 5 mm. All patients received abdominal CT prior to emergency surgery, revealing dilated loops and transition points. Two radiologists, each with over ten years of experience and blinded to clinical details, independently evaluated the CT images.

Clinical model construction

Univariate analyses were conducted to compare clinical characteristics, including clinical data, laboratory parameters, and CT findings, between patients who underwent surgical resection and those who did not, using the training set. A multilayer perceptron (MLP) network classifier and logistic regression (LR) were used to develop the clinical model, incorporating significant factors identified through univariate regression. Odds ratios (ORs) and 95% confidence intervals (CIs) were calculated to estimate the relative risks associated with independent factors.

Image segmentation and extraction of Radiomic features

The workflow of radiomics analysis is depicted in Fig. 1. The first step is volume of interest (VOI) segmentation. Three-dimensional volume rendering was used to

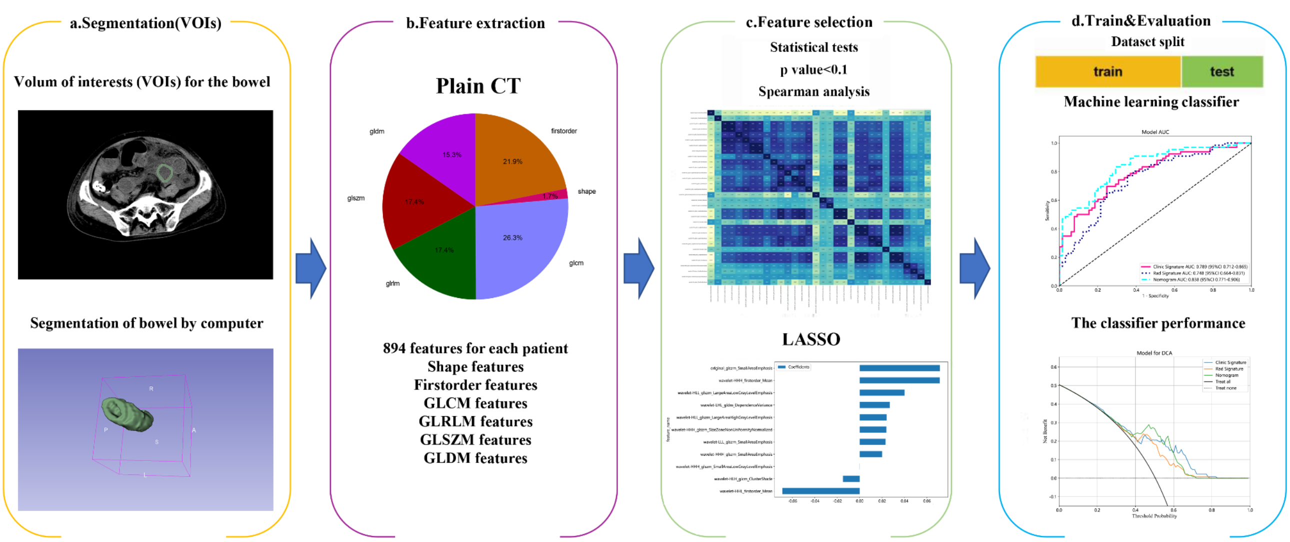

Fig. 1 Workflow to predict surgical resection in ASBO patients utilizing CT radiomics. The process comprises four steps: (**A**) Lesion segmentation, (**B**) Feature extraction, (**C**) Feature selection, and (**D**) Model construction and evaluation. CT: computed tomography; LASSO: least absolute shrinkage and selection operator

analyze the diseased bowel segments, providing greater flexibility than two-dimensional volume rendering [24]. Two experienced radiologists, unaware of clinical details, delineated the VOI within the bowel from axial CT images. Semiautomated threshold-based 3D Slicer software (version 4.11) was used for 3D segmentation, with contours drawn slice-by-slice at the transition zone between dilated small bowel and flat loops, ensuring minimal interference from surrounding structures. Two experienced radiologists meticulously outlined the contours of transition zone and adjacent lumen. This was done to evaluate inter-observer reproducibility. Subsequently, a senior radiologist reviewed the differing opinions and reached a consensus to define unified VOIs. The process of VOI segmentation for two representative patients is illustrated in Fig. 2, and the details are described in Supplementary materials A2. Radiomic features were extracted from the segmented VOIs using the 3D Slicer Radiomics Extension Pack (version 4.10.2). Features included shape, first-order statistics, and texture characteristics (e.g., gray level co-occurrence matrix (GLCM), gray level difference matrix (GLDM), gray level run-length matrix (GLRLM), and gray level size zone matrix (GLSZM)).

Radiomic signature construction

Stability and repeatability of feature extraction were assessed using interclass correlation coefficients (ICCs), and only features with ICCs greater than 0.75 were retained. Feature selection was based on the training cohort. To develop the radiomic signature, dimensionality reduction was performed to eliminate redundant features. Univariate analysis using the Wilcoxon test identified significant features with a p-value less than 0.1 in the training set. Spearman correlation analysis was conducted with a threshold of 0.9, and features were selected through pairwise comparison. The most significant features were identified using a least absolute shrinkage and selection operator (LASSO) regression algorithm. The radiomic signature was constructed using a multilayer perceptron (MLP) network classifier, with coefficients and intercept values used to calculate the Rad-score [25]. Details on the implementation of LASSO and MLP are given in the Supplementary Materials A3.

Radiomic Nomogram Construction and Verification

A multivariable logistic regression (LR) analysis was conducted to construct a radiomic-based nomogram, integrating significant clinical factors and Rad-scores to predict surgical resection. The nomogram's performance was assessed using calibration curves and the Hosmer–Lemeshow test. Decision curve analysis (DCA) was used to evaluate clinical efficacy at various threshold probabilities in both cohorts. Model performance was assessed with receiver operating characteristic (ROC) curves, AUC values, and measures of sensitivity, specificity, and accuracy.

Statistical analysis

Statistical analyses were performed using R software version 4.0.4 (https://www.r-project.org) and SPSS version 25.0. The Kolmogorov–Smirnov test assessed the normal

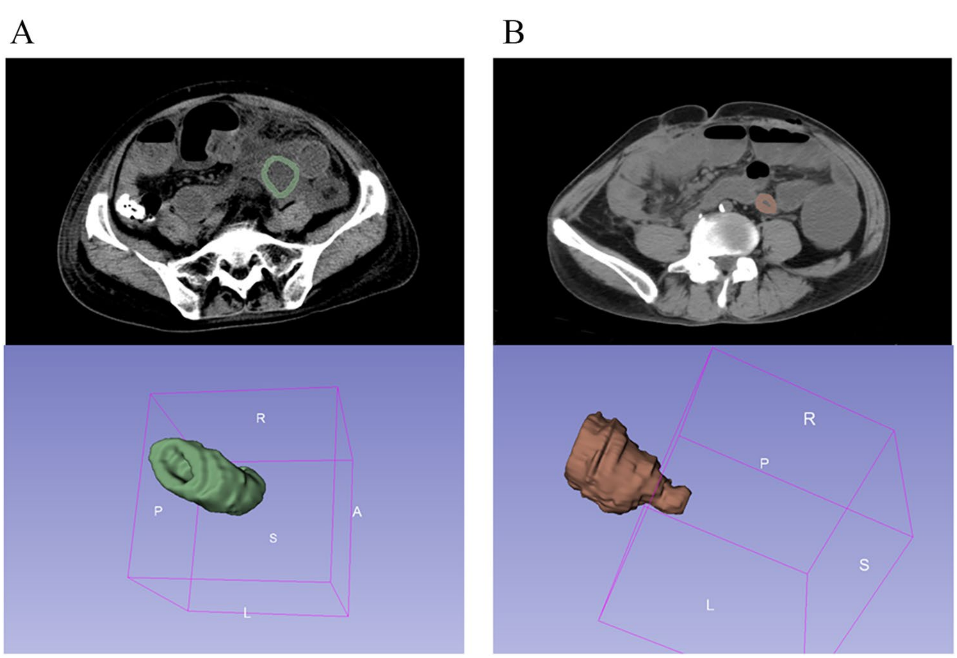

Fig. 2 Segmentation of the transition zone and nearby lumen, prone to ischemia. (**A**) Case 1: Manual three-dimensional segmentation in an ASBO patient not undergoing surgical resection. (**B**) Case 2: Manual three-dimensional segmentation in an ASBO patient who underwent surgical resection

distribution of texture features. Categorical data were analyzed with Chi-square and Fisher's exact tests, while continuous data were assessed using independent-sample t-tests. Non-normally distributed features were analyzed with the Mann–Whitney U test. The "glmnet" package in R was used for LASSO regression, and the "rms" package was employed to generate ROC curves, the nomogram, and calibration curves. The "rmda" package was used for decision curve analysis. A p-value of less than 0.05 was considered statistically significant.

Results

Patient characteristics

The detailed demographic data are presented in Table 1. In the training cohort, 66 out of 131 patients (50.38%) and in the test cohort, 26 out of 57 patients (45.61%) required surgical resection. The characteristics, including gender, age, BMI, and clinical manifestations, were comparable between the resection and non-resection groups in both cohorts. A higher proportion of patients with preoperative abdominal sepsis signs was observed in the resection group of the training cohort (56.06% vs. 38.46%, $p=0.044$); however, no significant differences were observed in the test cohort ($p=0.236$). CRP values were not statistically different in the training cohort but

Table 1 Clinical characteristics of patients in this study

	Training cohort		*p*	Test cohort		*p*
	Resection group ($n=66$)	Non-resection group ($n=65$)		Resection group ($n=26$)	Non-resection group ($n=31$)	
Age (years), mean (SD)	61.58 (14.45)	61.92 (13.05)	0.885	66.27 (12.73)	61.35 (13.95)	0.174
Gender, n (%)			0.923			0.646
Male	36 (54.55%)	36 (55.38%)		11 (42.31%)	15 (48.39%)	
Female	30 (45.45%)	29 (44.62%)		15 (57.69%)	16 (51.61%)	
BMI (kg/m^2), mean (SD)	21.89 (3.14)	21.59 (3.02)	0.580	21.42 (2.99)	21.57 (3.22)	0.858
Abdominal sepsis signs, n (%)	37 (56.06%)	25 (38.46%)	0.044*	15 (57.69%)	13 (41.94%)	0.236
Fever	25 (37.88%)	17 (26.15%)		11 (42.31%)	10 (32.26%)	
Tachycardia	20 (30.30%)	14 (21.54%)		7 (26.92%)	7 (22.58%)	
Peritonitis	28 (42.42%)	20 (30.77%)		10 (38.46%)	10 (32.26%)	
Manifestations						
Obstruction time (d), mean (SD)	6.42 (7.32)	9.77 (14.09)	0.092	6.29 (7.80)	6.42 (6.33)	0.944
Previous abdominal surgery, mean (SD)	1.03 (0.61)	1.05 (0.76)	0.895	1.12 (1.10)	1.23 (0.62)	0.637
Vomit, n (%)	44 (66.67%)	37 (56.92%)	0.521	21 (80.77%)	23 (74.19%)	0.556
Abdominal pain, n (%)	63 (95.45%)	59 (90.77%)	0.289	24 (92.31%)	30 (96.77%)	0.452
Abdominal distention, n (%)	48 (72.73%)	51 (78.46%)	0.445	22 (84.62%)	24 (77.42%)	0.493
No exhaust or defecation, n (%)	37 (56.06%)	35 (53.85%)	0.799	15 (57.69%)	17 (54.84%)	0.829
ASA score, mean (SD)	2.89 (0.08)	2.82 (0.08)	0.504	2.92 (0.39)	2.74 (0.51)	0.147
Laboratory values						
HB (g/L), mean (SD)	122.26 (20.21)	117.43 (20.63)	0.179	110.26 (27.78)	119.39 (19.46)	0.151
WBC (×10^9/L), mean (SD)	9.04 (7.04)	7.17 (3.83)	0.062	6.30 (2.56)	6.07 (2.26)	0.723
CRP (mg/L), mean (SD)	40.27 (54.93)	32.70 (40.58)	0.371	41.82 (47.55)	18.38 (24.01)	0.029*
PLT (×10^9/L), mean (SD)	244.94 (83.61)	254.86 (81.41)	0.493	214.46 (66.78)	234.61 (69.77)	0.273
ALB (g/L), mean (SD)	34.68 (5.99)	35.76 (6.00)	0.303	34.37 (6.97)	34.66 (6.29)	0.872
CT findings, n (%)						
Elevated wall density	19 (28.79%)	8 (12.31%)	0.020*	5 (19.23%)	2 (6.45%)	0.143
Thickened bowel	34 (51.52%)	17 (26.15%)	0.003*	13 (50.00%)	9 (29.03%)	0.105
Ascites	46 (69.70%)	23 (35.38%)	0.001*	19 (73.08%)	11 (35.48%)	0.005*
Mesenteric fluid	42 (63.64%)	21 (32.31%)	0.001*	13 (50.00%)	8 (25.81%)	0.059
Bowel wall gas	20 (30.30%)	9 (13.85)	0.023*	7 (26.92%)	1 (3.23%)	0.010*
Free air	5 (7.58%)	5 (7.70%)	0.980	2 (7.69%)	0	0.116
Small bowel feces sign	26 (39.39%)	13(20.00%)	0.015*	8 (30.77%)	6 (19.35%)	0.319
Whirlpool sign	9 (13.64%)	6 (9.23%)	0.428	4 (15.38%)	4 (12.90%)	0.788
Hypertension of mesenteric fat	16 (24.24%)	6 (9.23%)	0.022*	4 (15.38%)	3 (9.68%)	0.513

Note: *p<0.05

BMI, body mass index; ASA, American Society of Anesthesiologists; HB, hemoglobin; WBC, white blood cell; CRP, C-reactive protein; PLT, platelet; ALB, albumin showed a higher trend in the resection group of the test cohort ($p = 0.029$). Only two clinical factors identified by univariate analysis, ascites and bowel wall gas, also showed significant differences in the test cohort (Table 2, $p < 0.05$). Operation-related details are presented in Supplementary Table S4.

Multivariate analysis and clinical Model Development

In the multivariable analysis (Table 2), clinical factors showing slight differences in the training cohort ($p < 0.1$), including obstruction time, WBC count, and preoperative sepsis signs (i.e., fever, tachycardia, peritonitis), along with CT findings of elevated wall density, thickened wall, mesenteric fluid, ascites, bowel wall gas, small bowel feces, and hyperdensity of mesenteric fat, were included. These ten clinical features were analyzed using the MLP network classifier to construct one MLP clinical factor model. Binary logistic regression analysis confirmed that only thickened bowel wall (OR = 2.518, 95% CI: 1.056–6.003, $p = 0.037$) and ascites (OR = 3.931, 95% CI: 1.100-14.039, $p = 0.035$) were significantly associated with surgical resection in the training cohort and were used to build a logistic regression model. By comparing LR and MLP models, we found the latter performed better (Supplementary Table S5), thus we chose MLP model to build the fusion model furtherly.

Radiomic features and Radiomic signature construction

A total of 894 radiomic features were extracted from the VOIs of plain CT images. Univariate analysis revealed significant differences in features with an ICC > 0.75 between patients who underwent surgical resection and those who did not. The remaining features were selected via Spearman correlation analysis and were included in the LASSO regression model to determine the most important features. The optimal regularization parameter λ was identified using a 10-fold cross-validation with the R package (Fig. 3). Ultimately, an MLP network classifier was employed to construct the radiomic signature with 11 selected features (Table 3). The AUCs of the radiomic signature were 0.748 (95% CI, 0.664–0.831) for the training cohort and 0.728 (95% CI, 0.587–0.869) for the test cohort (Table 4).

Radiomic Nomogram Construction, Verification, and Model Assessment

A radiomic nomogram, based on the logistic regression model and incorporating both the radiomic signature and clinical factor model, was constructed. The calibration curve showed favorable agreement in both cohorts (Fig. 4). The AUC values of the radiomic nomogram for distinguishing surgical resection risk were 0.838 (95% CI, 0.771–0.906) for the training cohort and 0.761 (95% CI, 0.628–0.893) for the test cohort, indicating significant improvements compared to using the radiomic signature or clinical model alone (Fig. 5; Table 4). Furthermore, when the clinical model was combined with radiomic signatures, the sensitivity and negative predictive value (NPV) for the test cohort reached 0.769 and 0.786, respectively, which were higher than those achieved by the clinical and radiomics models alone. According to decision curve analysis (DCA) curves, our constructed nomogram achieved better net benefits than the clinical model or radiomic signature at optimal threshold probabilities in predicting surgical resection in acute ASBO cases.

Discussion

The early and accurate identification of ASBO patients requiring surgical resection remains a topic of ongoing debate. Our study demonstrates that integrating radiomic features with clinically relevant factors provides a robust tool for predicting the risk of surgical resection in ASBO patients. This is the first clinical model to combine CT radiomic features from affected bowel segments with clinical data, offering superior predictive accuracy compared to models relying solely on clinical or radiomic

Table 2 Univariate and multivariate analysis of patients with surgical resection versus those without in the training cohort

	Univariate analysis				Multivariate analysis			
	SE	OR	*p* value	95% CI	SE	OR	*p* value	95% CI
Abdominal sepsis signs	0.356	2.041	0.045	1.017–4.099	0.419	1.736	0.188	0.764–3.945
Obstruction time	0.018	0.971	0.093	0.938–1.006	0.019	0.975	0.187	0.939–1.012
WBC counts	0.037	1.068	0.077	0.093–1.149	0.043	1.029	0.499	0.947–1.119
Elevated wall density	0.465	2.880	0.023	1.157–7.169	0.634	1.939	0.296	0.560–6.721
Thickened bowel	0.375	3.000	0.003	1.440–6.251	0.443	2.518	0.037	1.056–6.003
Ascites	0.373	4.200	0.001	2.022–8.722	0.650	3.931	0.035	1.100-14.039
Mesenteric fluid	0.369	3.667	0.001	1.781–7.550	0.655	1.069	0.919	0.296–3.858
Bowel wall gas	0.448	2.705	0.026	1.124–6.510	0.528	1.337	0.582	0.475–3.765
Small bowel feces sign	0.400	2.600	0.017	1.188–5.689	0.499	2.246	0.105	0.845–5.969
Hypertension of mesenteric fat	0.516	3.147	0.026	1.145–8.649	0.707	2.396	0.217	0.599–9.586

Note: BMI, body mass index; ASA, American Society of Anesthesiologists; HB, hemoglobin; WBC, white blood cell; CRP, C-reactive protein; PLT, platelet; ALB, albumin

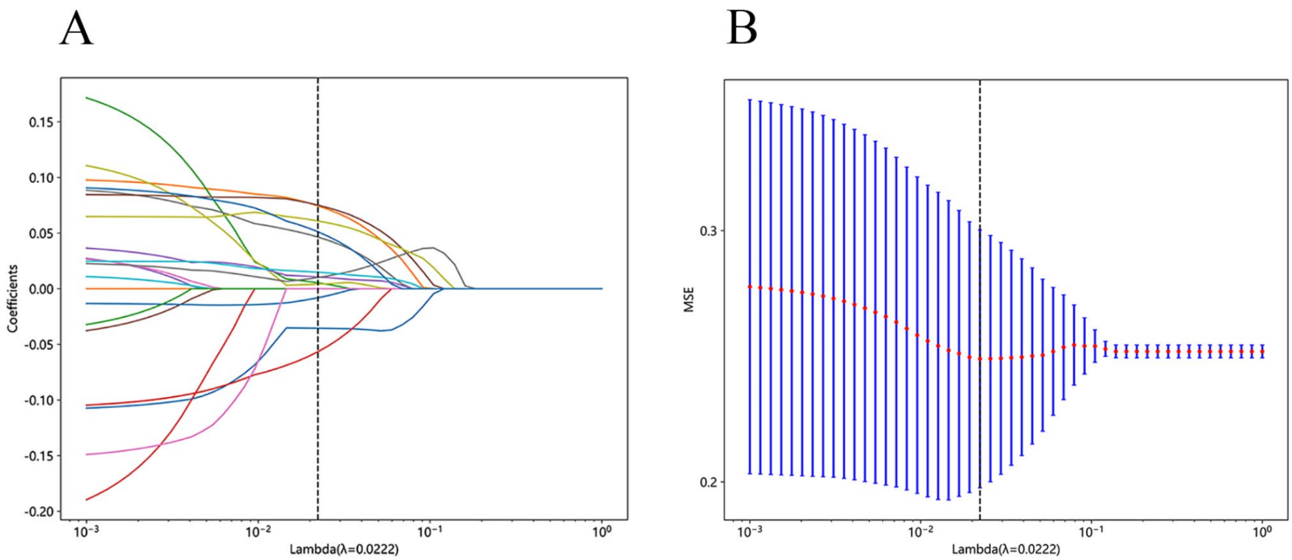

Fig. 3 Selection of radiomic features utilizing the LASSO regression model. (**A**) Determination of the tuning parameter (λ) through cross-validation employing the 1-standard error rule. Dotted vertical lines demarcate the optimal λ values. (**B**) Coefficient profile diagram displaying the link between the coefficients and the chosen log λ value via tenfold cross-validation

Table 3 Radiomics feature selection results

Variables	Radiomics feature name
A	original-glszm-SmallAreaEmphasis
B	wavelet-HHH-firstorder-Mean
C	wavelet-HLL-glszm-LargeAreaLowGrayLevelEmphasis
D	wavelet-LHL-gldm-DependenceVariance
E	wavelet-HLL-glszm-LargeAreaHighGrayLevelEmphasis
F	wavelet-HHH-glszm-SizeZoneNonUniformityNormalized
G	wavelet-LLL-glszm-SmallAreaEmphasis
H	wavelet-HHH-glszm-SmallAreaEmphasis
I	wavelet-HHH-glszm-SmallAreaLowGrayLevelEmphasis
J	wavelet-HLH-glcm-ClusterShade
K	wavelet-HHL-firstorder-Mean

Note: glszm, gray level size zone matrix; gldm, gray level difference matrix; glcm, gray level co-occurrence matrix.

factors. This integrated approach has the potential to significantly enhance clinical decision-making.

Unlike previous studies that compared operative and non-operative management of ASBO [10–14], our cohort exclusively comprised patients who underwent surgical intervention. The surgical resection rates in our study are 50.38% in the training group and 45.61% in the test group, which are higher than the 28–45.7% reported in the literature [5–7, 26]. This discrepancy is likely due to the tertiary nature of our center, which handles a higher volume of critically ill patients transferred from other facilities. Many ASBO patients undergo 3–4 days of conservative treatment before being transferred to our institution for surgical intervention, resulting in a total treatment duration of approximately 6–9 days. Consequently, these patients often present with more severe clinical manifestations, including prolonged obstruction, complex comorbidities, and, frequently, infectious complications. However, those for whom conservative measures fail are typically referred to our tertiary center for further evaluation and ultimate surgical management. This referral process might introduce selection bias into the current study. Future large-scale studies should aim to include more patients who are initially treated with successful conservative therapy. Our findings are consistent with previous research indicating that preoperative infections, such as fever, tachycardia, and peritonitis, are more prevalent among patients undergoing surgical resection [27]. Signs of peritonitis, including guarding, rebound tenderness, and abdominal rigidity, often suggest advanced deterioration, such as transmural ischemia or bowel perforation, which significantly predicts bowel strangulation [28]. However, our study did not find significant diagnostic efficacy from various laboratory biomarkers, possibly due to the complex pathophysiology of mucosal hypoxia and transmural infection. Existing biomarkers have not yet achieved reliable diagnostic accuracy for the early detection of intestinal ischemia [29]. Additionally, all subjects in this study underwent operations under the suspicion of bowel ischemia in emergent settings, likely sharing a common profile of inflammatory biomarkers. In this study, we found that clinical signs suggesting pronounced septic physiology and infection should be promptly investigated, regardless of laboratory test results, aligning with Evennett's conclusion that serological markers are suboptimal for routine clinical use [30].

CT scanning remains a prevalent diagnostic tool for determining the cause and severity of ASBO. Our study confirms that certain CT signs are significantly associated

Table 4 Predictive performance of the three models in the training and test sets

	Training cohort ($n=131$)						Testing cohort ($n=57$)					
	AUC (95% CI)	**ACC**	**SEN**	**SPE**	**PPV**	**NPV**	**AUC (95% CI)**	**ACC**	**SEN**	**SPE**	**PPV**	**NPV**
Clinical model	0.789 (0.712–0.865)	0.725	0.697	0.754	0.742	0.710	0.679 (0.534–0.823)	0.702	0.731	0.677	0.655	0.750
Radiomic signature	0.748 (0.664–0.831)	0.710	0.773	0.646	0.689	0.737	0.728 (0.587–0.869)	0.772	0.731	0.806	0.760	0.781
Nomogram	0.838 (0.771–0.906)	0.771	0.833	0.708	0.743	0.807	0.761 (0.628–0.893)	0.737	0.769	0.710	0.690	0.786

Note: AUC, area under the curve; CI, confidence interval; ACC, accuracy; SEN, sensitivity; SPE, specificity; PPV, positive predictive value; NPV, negative predictive value

with the need for surgical resection, consistent with previous findings. While CT angiography (CTA) is often considered the gold standard for diagnosing bowel ischemia [31], its use is limited by the risk of contrast-induced nephropathy, high costs, and availability constraints [32]. In practice, plain CT scanning is often more feasible, and our analysis of plain CT images effectively assessed the risk of surgical resection. Seven CT signs, including elevated wall density, thickened bowel wall, ascites, mesenteric fluid, bowel wall gas, small bowel feces, and hyperdensity of mesenteric fat, were significantly correlated with the need for surgical resection. While signs like ascites can indicate strangulation, they are not definitive, as ascites can also result from other conditions such as tumors or liver disease [33, 34]. Furthermore, in a multi-institution prospective study by Kulvatunyou et al., the positive predictive values (PPVs) of each CT finding were relatively low in predicting surgical intervention [35]. Similarly, Kupietzky and colleagues validated three existing clinical-radiographic scores designed to predict the risk of ischemia and demonstrated that these scores had been overestimated in an independent cohort of surgical patients, yielding a PPV of 8.3–28.5%, which was relatively low [36]. The effectiveness of clinical models is largely restricted by the subjective interpretation of clinicians and radiologists. Given the limitations of CT imaging, we propose a novel approach for predicting surgical resection using new radiomic parameters based on CT data.

The advancement of radiomics has been substantially propelled by progress in pattern recognition methods and the refinement of quantitative imaging features, demonstrating considerable promise in providing computational imaging measurements relevant to gastrointestinal diseases [16]. Identifying CT image signs associated with bowel resection in ASBO patients is both labor-intensive and time-consuming, making it impractical for emergency situations. In contrast, radiomics facilitates the extraction of high-throughput features from radiographic images that capture molecular heterogeneity invisible to the human eye [37]. For instance, Chirra et al. developed a radiomics-based machine-learning model to characterize the degree of intestinal inflammation and fibrosis in CD strictures, successfully elucidating the pathophysiological basis of the radiomic features [38]. Similarly, Tian Yang et al. investigated pancreatic radiomics to predict treatment responses to infliximab in biologic-naive CD patients [39]. Li et al. constructed a CT-based radiomic nomogram using data from 165 lesions in 87 patients to differentiate between ulcerative colitis and Crohn's disease [40]. Our previous work combined radiomic features from the lumen and mesentery to develop a model for identifying moderate-to-severe CD and predicting its surgical progression [18]. Unlike

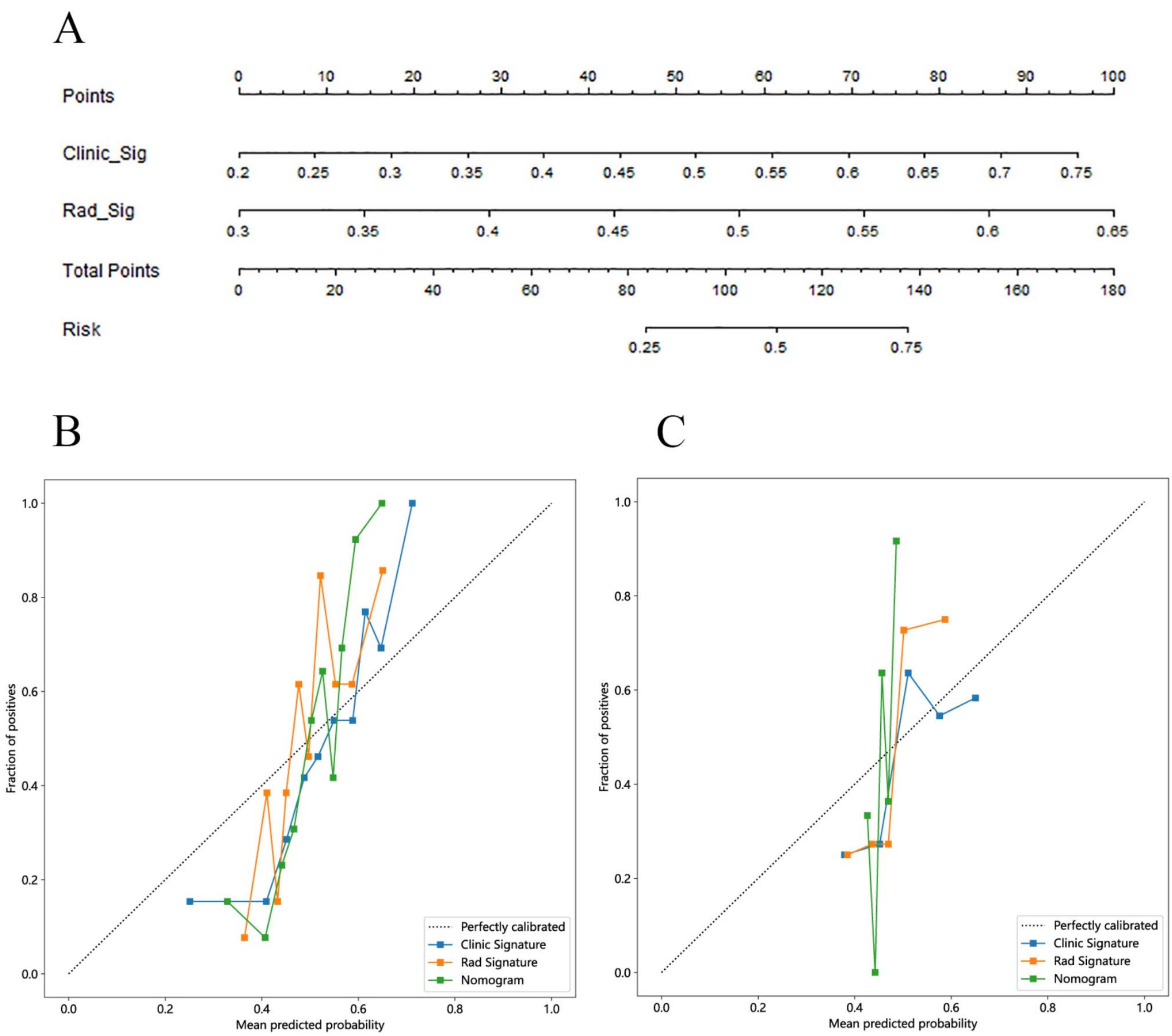

Fig. 4 Development and calibration of the radiomic nomogram. (**A**) Formulation of the radiomic nomogram within the training group, incorporating clinical indicators and Rad-score. The calibration curves displayed for both the training (**B**) and testing (**C**) cohorts highlight the model's fit

earlier studies, our research highlights the application of radiomics in analyzing diseased bowel segments and its predictive value for clinical use. Given the associations between transition zone and surgical resection risk, eleven radiomic features were selected in current study, including one original and ten wavelet indices measuring mean, minimum, maximum, and standard deviation values within the VOIs. Wavelet features, obtained from wavelet transform techniques, capture texture information by analyzing pixel intensity variations at different scales and orientations, revealing subtle tissue changes that might be missed in the original image [41]. Our radiomics model, based primarily on wavelet features and constructed using a modern feedforward artificial neural network (MLP), showed significant improvements in AUC and PPV in the test cohort, offering valuable support for clinicians in interpreting intestinal conditions. The MLP outperformed the LR due to its ability to model complex, non-linear relationships in the data, capturing interactions that LR could not. Unlike LR, which assumes a linear relationship, the MLP utilizes multiple layers to learn intricate patterns, making it better suited for tasks involving complex feature interactions, such as radiomic data. The performance difference was evaluated using accuracy, AUC, and PPV, with the MLP demonstrating superior predictive performance in identifying patients who require bowel resection.

By combining clinical factors and radiomic features, the nomogram provides a risk assessment for surgical bowel resection, which can facilitate timely and evidence-based

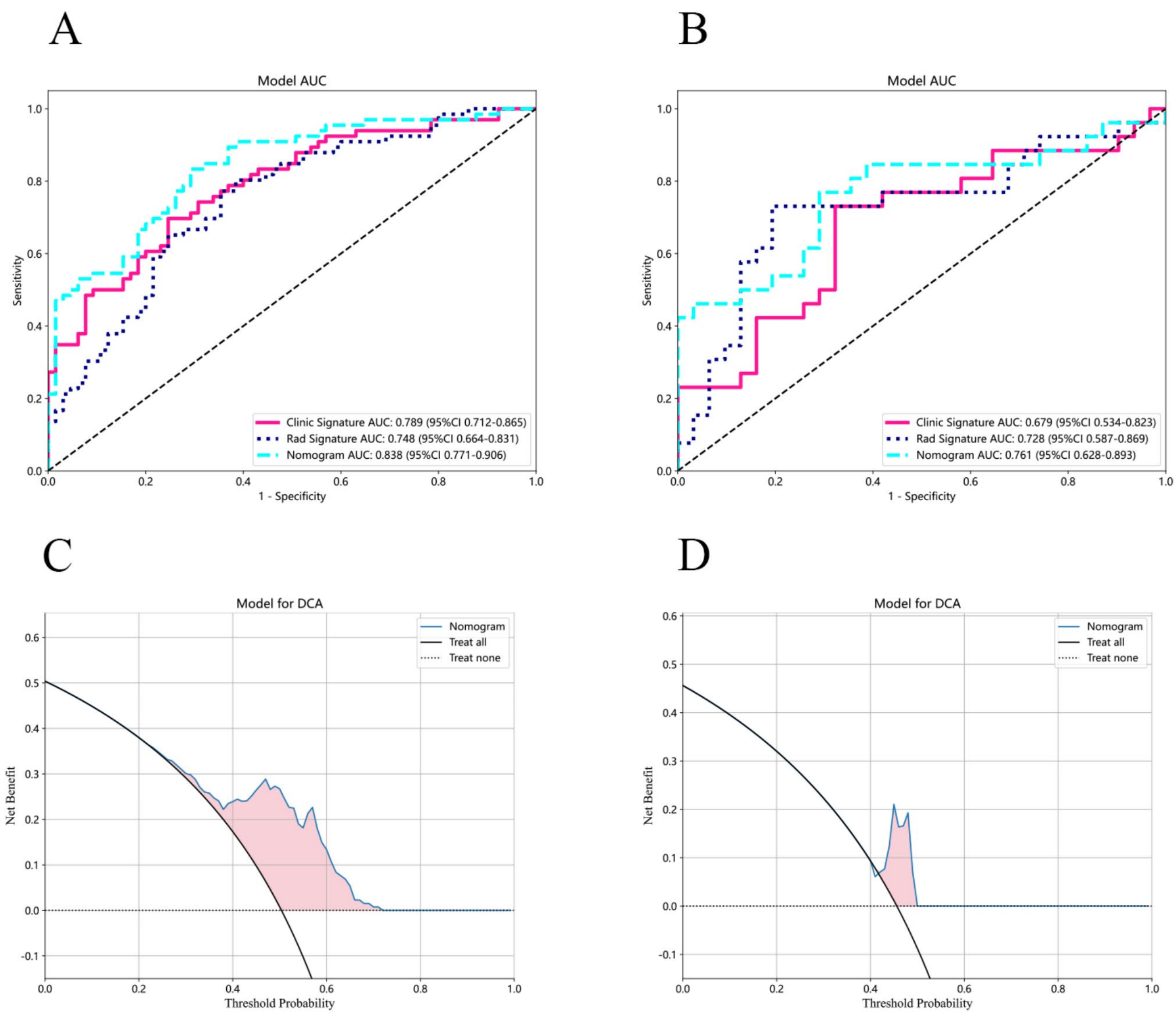

Fig. 5 ROC curves for the clinical model, radiomic signature, and combined radiomic nomogram within the training (**A**) and testing (**B**) groups. Decision curve analysis for the radiomic nomogram is conducted for both the training (**C**) and testing (**D**) cohorts

decision-making. For example, in the case of a 51-year-old woman with a 1-day history of bowel obstruction, a WBC count of 16.11×10^9/L, and CT findings of bowel thickening and ascites, the Rad-score was 63 and the Clinic-score was 69, resulting in a total risk score of 132, corresponding to a 69% probability of requiring bowel resection. This patient ultimately underwent bowel resection. In contrast, a 72-year-old man with a 6-day history of obstruction, a WBC count of 7.79×10^9/L, and lower Rad- and Clinic-scores resulted in a total risk score of 86, indicating a 28% likelihood of requiring resection (Supplementary Figure S3). In this case, adhesiolysis was performed instead of resection. These case examples demonstrate the potential clinical utility of the nomogram in guiding surgical decision-making. The ability to rapidly compute a personalized risk score, based on both radiomic and clinical factors, is especially valuable in emergency settings where timely decisions regarding surgical intervention are critical. Additionally, the model can enhance triage processes, improve medical resource allocation, and assist in the communication of treatment options to both patients and their families, fostering more informed and collaborative decision-making. What' more, the future development of a deep learning model for automatic segmentation of CT images could further enhance the extraction of radiomic features and the assessment of surgical resection risk in ASBO patients.

In this study, we designed and validated an integrated model that combines clinical and radiomic features. This fusion model exhibited a significantly higher AUC value compared to models that employed either clinical or radiomic features alone. In scenarios involving strangulated ASBO, where timely surgical interventions are imperative, the consequences of delay can be fatal. Medical professionals often give precedence to the sensitivity of diagnostic tools in detecting intestinal ischemia. When necrotic bowel is suspected, surgeons generally opt for laparotomy. Our findings reveal that the radiomic nomogram outperforms other models in terms of sensitivity and negative predictive value in testing phases, indicating its superior applicability for ASBO cases. Thus, the fusion nomogram emerges as a dependable and precise instrument for delivering clinical data, enhancing time efficiency, and aiding in clinical decision-making processes.

One significant hurdle encountered in this research was the delineation of VOIs. To the best of our knowledge, no previous studies have investigated segmentation techniques based on CT plain images specifically for ASBO patients. Due to the intestines' variable shapes and movements, stringent criteria must be applied to guarantee the high quality of images necessary for precise lesion identification and segmentation. The segment of the bowel requiring resection was evaluated at the transition between normal and dilated sections by two radiologists, each with over a decade of experience. The accumulation of fluids, feces, and gas at this junction can escalate intestinal pressure, diminish wall thickness, compromise blood supply, and necessitate surgical resection. Interpreting CT features that suggest the need for surgical intervention poses a challenge to less experienced surgeons and radiologists, emphasizing the importance of extensive experience and meticulous examination. Radiomics introduces an innovative method by quantifying image characteristics to provide objective data, transcending the limitations of macroscopic evaluations and boosting the accuracy and dependability of surgical prognostications.

Despite the promising findings of this study, several limitations should be considered. First, the use of data from a single institution limits the generalizability of our results. Multicenter studies with larger, more diverse sample sizes are needed to validate and strengthen our conclusions. Additionally, the case studies were sourced from the emergency department, and the radiomic model was developed using plain CT images. Future research should explore the potential benefits of contrast-enhanced CT scans, which may provide more detailed imaging and enhance the model's applicability in broader clinical settings. Another limitation is the risk of overfitting, where the MLP may perform well on the training dataset but struggle to generalize effectively to the test datasets. This concern is particularly pertinent due to the relatively small sample size in this study.

Conclusion

In summary, this research effectively established and corroborated a nomogram that combines radiomic with clinical data to forecast surgical resection for ASBO patients. This method markedly enhances diagnostic precision relative to conventional radiographic techniques, and aids clinicians in forming better-informed decisions.

Supplementary Information

The online version contains supplementary material available at https://doi.org/10.1186/s12880-025-01575-7.

Supplementary Material 1

Supplementary Material 2

Supplementary Material 3

Acknowledgements

None.

Author contributions

Zhibo Wang, Shunli Liu, Yuxi Wang, and Ruiqing Liu wrote the main manuscript. Ling Zhu, Dalue Li, Jingnong Liu, and Xiaoming Zhou prepared figures and tables. All authors reviewed the manuscript.

Funding

This research was supported by the National Natural Science Foundation of China (82000482, 82402383), China Postdoctoral Science Foundation funded (No. 2023M741858), Beijing Xisike Clinical Oncology Research Foundation (Y-NESTLE2022QN-0230) and China Crohn's & Colitis Foundation (CCCF) (CCCF-QF-2023C18-3).

Data availability

The datasets used and analysed during the current study are available from the corresponding author on reasonable request.

Declarations

Ethics approval and consent to participate

The Ethics Committee of the Affiliated Hospital of Qingdao University approved the study (QYFYWZLL26445). Due to the nature of the study, which involved analysis of pre-existing data, written informed consent was waived by Ethics Committee of the Affiliated Hospital of Qingdao University.

Consent for publication

N/A.

Competing interests

The authors declare no competing interests.

Author details

[1]Department of Gastrointestinal Surgery, The Affiliated Hospital of Qingdao University, Qingdao 266003, China
[2]Department of General Surgery, Weifang People's hospital, Weifang 261000, China
[3]Shandong Key Laboratory of Digital Medicine and Computer Assisted Surgery, The Affiliated Hospital of Qingdao University, Qingdao 266003, China
[4]Department of Radiology, The Affiliated Hospital of Qingdao University, Qingdao 266003, China
[5]Emergency Department, The Affiliated Hospital of Qingdao University, Qingdao 266003, China
[6]Acute Abdomen Surgery Department, The second hospital of Dalian medical university, Dalian 116027, China
[7]The Affiliated Hospital of Qingdao University, Wutaishan-road No.1677, Qingdao 266071, Shandong, China

Received: 30 September 2024 / Accepted: 28 January 2025
Published online: 11 February 2025

References

1. Behman R, Nathens AB, Mason S, et al. Association of Surgical Intervention for Adhesive Small-Bowel Obstruction with the risk of recurrence. JAMA Surg. 2019;154(5):413–20. https://doi.org/10.1001/jamasurg.2018.5248.
2. Maheta BJ, Manhas P, Niu A, et al. What should I use? Impact of adhesion barriers on postoperative abdominal complications: a systematic review. Am Surg. 2024 May;25:31348241258718. https://doi.org/10.1177/00031348241258718.
3. ten Broek RP, Issa Y, van Santbrink EJ, et al. Burden of adhesions in abdominal and pelvic surgery: systematic review and met-analysis. BMJ. 2013;347:f5588. https://doi.org/10.1136/bmj.f5588.
4. Lasithiotakis K, Kritsotakis EI, Kokkinakis S, et al. The Hellenic Emergency Laparotomy Study (HELAS): a prospective Multicentre Study on the Outcomes of Emergency Laparotomy in Greece. World J Surg. 2023;47(1):130–9. https://doi.org/10.1007/s00268-022-06723-6.
5. Carr MJ, Badiee J, Benham DA, et al. Surgical management and outcomes of adhesive small bowel obstruction: teaching versus non-teaching hospitals. Eur J Trauma Emerg Surg. 2022;48(1):107–12. https://doi.org/10.1007/s00068-021-01812-y.
6. Chin RL, Lima DL, Pereira X, et al. Assessing outcomes in laparoscopic vs open surgical management of adhesive small bowel obstruction. Surg Endosc. 2023;37(2):1376–83. https://doi.org/10.1007/s00464-022-09314-7.
7. Symer MM, Zheng X, Pua BB, et al. Contemporary Assessment of Adhesiolysis and Resection for Adhesive small bowel obstruction in the state of New York. Surg Innov. 2024;31(3):245–55. https://doi.org/10.1177/15533506241240580.
8. Wang Z, Sun B, Yu Y, et al. A novel nomogram integrating body composition and inflammatory-nutritional markers for predicting postoperative complications in patients with adhesive small bowel obstruction. Front Nutr. 2024;11:1345570. https://doi.org/10.3389/fnut.2024.1345570.
9. Scaglione M, Galluzzo M, Santucci D, et al. Small bowel obstruction and intestinal ischemia: emphasizing the role of MDCT in the management decision process. Abdom Radiol (NY). 2022;47(5):1541–55. https://doi.org/10.1007/s00261-020-02800-3.
10. Diamond M, Lee J, LeBedis CA. Small bowel obstruction and ischemia. Radiol Clin North Am. 2019;57(4):689–703. https://doi.org/10.1016/j.rcl.2019.02.002.
11. Millet I, Taourel P, Ruyer A, et al. Value of CT findings to predict surgical ischemia in small bowel obstruction: a systematic review and meta-analysis. Eur Radiol. 2015;25(6):1823–35. https://doi.org/10.1007/s00330-014-3440-2.
12. Sheedy SP, Earnest F 4th, Fletcher JG, et al. CT of small-bowel ischemia associated with obstruction in emergency department patients: diagnostic performance evaluation. Radiology. 2006;241(3):729–36. https://doi.org/10.1148/radiol.2413050965.
13. Matsushima K, Inaba K, Dollbaum R, et al. High-density free fluid on computed tomography: a predictor of Surgical intervention in patients with Adhesive small bowel obstruction. J GastVOIntest Surg. 2016;20(11):1861–6. https://doi.org/10.1007/s11605-016-3244-6.
14. Jang KM, Min K, Kim MJ, et al. Diagnostic performance of CT in the detection of intestinal ischemia associated with small-bowel obstruction using maximal attenuation of region of interest. AJR Am J Roentgenol. 2010;194(4):957–63. https://doi.org/10.2214/AJR.09.2702.
15. Kobayashi T, Chiba N, Koganezawa I, et al. Prediction model for irreversible intestinal ischemia in strangulated bowel obstruction. BMC Surg. 2022;22(1):321. https://doi.org/10.1186/s12893-022-01769-8.
16. Bülbül HM, Burakgazi G, Kesimal U, et al. Radiomics-based machine learning in the differentiation of benign and malignant bowel wall thickening radiomics in bowel wall thickening. Jpn J Radiol. 2024;42(8):872–9. https://doi.org/10.1007/s11604-024-01558-8.
17. Wang L, Gong J, Huang X, et al. CT-based radiomics nomogram for preoperative prediction of 10 lymph nodes metastasis in advanced proximal gastric cancer. Eur J Surg Oncol. 2021;47(6):1458–65. https://doi.org/10.1016/j.ejso.2020.11.132.
18. Ruiqing L, Jing Y, Shunli L, et al. A Novel Radiomics Model integrating Luminal and Mesenteric features to predict mucosal activity and surgery risk in Crohn's Disease patients: a Multicenter Study. Acad Radiol. 2023;30(Suppl 1):S207–19. https://doi.org/10.1016/j.acra.2023.03.023.
19. Li X, Liang D, Meng J, et al. Development and Test of a Novel computed-tomography Enterography Radiomic Approach for characterization of Intestinal Fibrosis in Crohn's Disease. Gastroenterology. 2021;160(7):2303–e231611. https://doi.org/10.1053/j.gastro.2021.02.027.
20. Kocak B, Baessler B, Bakas S, et al. CheckList for EvaluAtion of Radiomics research (CLEAR): a step-by-step reporting guideline for authors and reviewers endorsed by ESR and EuSoMII. Insights Imaging. 2023;14(1):75. https://doi.org/10.1186/s13244-023-01415-8.
21. Kocak B, Akinci D'Antonoli T, Mercaldo N et al. METhodological RadiomICs Score (METRICS): a quality scoring tool for radiomics research endorsed by EuSoMII. Insights Imaging. 2024;15(1):8. Published 2024 Jan 17. https://doi.org/10.1186/s13244-023-01572-w
22. Pricolo VE, Curley F. CT scan findings do not predict outcome of nonoperative management in small bowel obstruction: retrospective analysis of 108 consecutive patients. Int J Surg. 2016;27:88–91. https://doi.org/10.1016/j.ijsu.2016.01.033.
23. Ferris B, Bastian-Jordan M, Fenwick J, et al. Vascular assessment in small bowel obstruction: can CT predict requirement for surgical intervention? Abdom Radiol (NY). 2021;46(2):517–25. https://doi.org/10.1007/s00261-020-02698-x.
24. Hong SS, Kim AY, Byun JH, et al. MDCT of small-bowel disease: value of 3D imaging. AJR Am J Roentgenol. 2006;187(5):1212–21. https://doi.org/10.2214/AJR.04.1762.
25. Jiang Z, Xie W, Zhou X, et al. A virtual biopsy study of microsatellite instability in gastric cancer based on deep learning radiomics. Insights Imaging. 2023;14(1):104. https://doi.org/10.1186/s13244-023-01438-1.
26. Zein L, Calame P, Chausset C, et al. Preoperative prediction of inadvertent surgical resection during adhesive small bowel obstruction surgery using combination of CT features. Eur Radiol. 2022;32(10):6646–57. https://doi.org/10.1007/s00330-022-08951-9.
27. Tsumura H, Ichikawa T, Hiyama E, et al. Systemic inflammatory response syndrome (SIRS) as a predictor of strangulated small bowel obstruction. Hepatogastroenterology. 2004 Sep-Oct;51(59):1393–6.
28. Eren T, Boluk S, Bayraktar B, et al. Surgical indicators for the operative treatment of acute mechanical intestinal obstruction due to adhesions. Ann Surg Treat Res. 2015;88(6):325–33. https://doi.org/10.4174/astr.2015.88.6.325.
29. Peoc'h K, Nuzzo A, Guedj K, et al. Diagnosis biomarkers in acute intestinal ischemic injury: so close, yet so far. Clin Chem Lab Med. 2018;56(3):373–85. https://doi.org/10.1515/cclm-2017-0291.
30. Evennett NJ, Petrov MS, Mittal A, et al. Systematic review and pooled estimates for the diagnostic accuracy of serological markers for intestinal ischemia. World J Surg. 2009;33(7):1374–83. https://doi.org/10.1007/s00268-009-0074-7.
31. Nakamura Y, Kondo S, Narita K, et al. Understanding CT imaging findings based on the underlying pathophysiology in patients with small bowel ischemia. Jpn J Radiol. 2023;41(4):353–66. https://doi.org/10.1007/s11604-022-01367-x.
32. Murray L, Foureau J-D, Boehm K et al. 36 effect of contrast dye on renal function of diabetics who presented with Acute Ischemic Stroke after computed-tomography Angiography Head and Neck. Annals of Emergency Medicine. 2023 Oct; 15:824.
33. Zielinski MD, Eiken PW, Bannon MP, et al. Small bowel obstruction-who needs an operation? A multivariate prediction model. World J Surg. 2010;34(5):910–9. https://doi.org/10.1007/s00268-010-0479-3.
34. Jones K, Mangram AJ, Lebron RA, et al. Can a computed tomography scoring system predict the need for surgery in small-bowel obstruction? Am J Surg. 2007;194(6):780–3. https://doi.org/10.1016/j.amjsurg.2007.09.020. discussion 783-4.
35. Kulvatunyou N, Pandit V, Moutamn S, et al. A multi-institution prospective observational study of small bowel obstruction: clinical and computerized tomography predictors of which patients may require early surgery. J Trauma Acute Care Surg. 2015;79(3):393–8. https://doi.org/10.1097/TA.0000000000000759.
36. Kupietzky A, Dodi O, Dover R, et al. Existing scores fail to Predict Bowel Ischemia in patients with Adhesive small bowel obstruction. J Surg Res. 2023;283:416–22. https://doi.org/10.1016/j.jss.2022.10.056.
37. Whybra P, Zwanenburg A, Andrearczyk V, et al. The image Biomarker Standardization Initiative: standardized Convolutional filters for reproducible Radiomics and enhanced clinical insights. Radiology. 2024;310(2):e231319. https://doi.org/10.1148/radiol.231319.
38. Chirra P, Sleiman J, Gandhi NS et al. Radiomics to Detect Inflammation and Fibrosis on Magnetic Resonance Enterography in Stricturing Crohn's Disease. J Crohns Colitis 2024 May 18: jjae073. https://doi.org/10.1093/ecco-jcc/jjae073

39. Yang T, Feng J, Yao R, et al. CT-based pancreatic radiomics predicts secondary loss of response to infliximab in biologically naïve patients with Crohn's disease. Insights Imaging. 2024;15(1):69. https://doi.org/10.1186/s13244-024-01637-4.
40. Li H, Mo Y, Huang C, et al. An MSCT-based radiomics nomogram combined with clinical factors can identify Crohn's disease and ulcerative colitis. Ann Transl Med. 2021;9(7):572. https://doi.org/10.21037/atm-21-1023.
41. Rahul K, Ankur G, Harkirat SA, et al. CGHF: a computational decision support system for glioma classification using hybrid Radiomics- and stationary wavelet-based features. IEEE Access. 2020 Apr;79440–58. https://doi.org/10.1109/ACCESS.2020.2989193.

Publisher's note